Functional genomic screen in mesothelioma reveals that loss of function of BRCA1-associated protein 1 induces chemoresistance to ribonucleotide reductase inhibition

Okonska, A.; Buhler, S.; Rao, V.; Ronner, M.; Blijlevens, M.; Meulen-Muileman, I.H. van der; ... ; Felley-Bosco, E.

Functional Genomic Screen in Mesothelioma Reveals that Loss of Function of BRCA1-Associated Protein 1 Induces Chemoresistance to Ribonucleotide Reductase Inhibition 🅐🅒

Agata Okonska[1], Saskja Bühler[1], Vasundhara Rao[1], Manuel Ronner[1], Maxime Blijlevens[2], Ida H. van der Meulen-Muileman[2], Renee X. de Menezes[3], Martin Wipplinger[1], Kathrin Oehl[4], Egbert F. Smit[5], Walter Weder[6], Rolf A. Stahel[7], Lorenza Penengo[8], Victor W. van Beusechem[2], and Emanuela Felley-Bosco[1]

ABSTRACT

Loss of function of BRCA1-associated protein 1 (BAP1) is observed in about 50% of malignant pleural mesothelioma (MPM) cases. The aim of this study was to investigate whether this aspect could be exploited for targeted therapy. A genetically engineered model was established expressing either functional or nonfunctional BAP1, and whole-genome siRNA synthetic lethality screens were performed assessing differentially impaired survival between the two cell lines. The whole-genome siRNA screen unexpectedly revealed 11 hits (FDR < 0.05) that were more cytotoxic to *BAP1*-proficient cells. Two actionable targets, ribonucleotide reductase (RNR) catalytic subunit M1 (RRM1) and RNR regulatory subunit M2 (RRM2), were validated. In line with the screen results, primary mesothelioma (*BAP1*$^{+/-}$) overexpressing *BAP1* C91A (catalytically dead mutant) was more resistant to RNR inhibition, while *BAP1* knockdown in the *BAP1*-proficient cell lines rescued the cells from their vulnerability to RNR depletion. Gemcitabine and hydroxyurea were more cytotoxic in *BAP1*-proficient cell line–derived spheroids compared with *BAP1* deficient. Upregulation of RRM2 upon gemcitabine and hydroxyurea treatment was more profound in *BAP1* mut/del cell lines. Increased lethality mediated by RNR inhibition was observed in NCI-H2452 cells reconstituted with *BAP1*-WT but not with *BAP1* C91A. Upregulation of RRM2 in NCI-H2452-*BAP1* WT spheroids was modest compared with control or C91A mutant. Together, we found that BAP1 is involved in the regulation of RNR levels during replication stress. Our observations reveal a potential clinical application where BAP1 status could serve as predictive or stratification biomarker for RNR inhibition-based therapy in MPM.

Introduction

Malignant pleural mesothelioma (MPM) is an aggressive cancer; clinical symptoms only appear at advanced disease and median survival is approximately 8 to 27 months depending on histotype and therapy (1). Thus, there is a significant need for new therapeutic approaches.

In the era of personalized medicine, one strategy is to investigate weaknesses that are dependent on mutated genes. Therefore, our original intention was to investigate synthetic lethality with mutated BRCA1-associated protein 1 (BAP1). BAP1 is the second most mutated gene in MPM (COSMIC, cancer.sanger.ac.uk V85) after *CDKN2A* (cyclin-dependent kinase inhibitor 2A) and loss of function of BAP1 has been reported in up to 50% of MPM (2).

BAP1 belongs to the group of deubiquitinating enzymes whose main function is the removal of ubiquitin entities from different targets, thereby opposing the function of E3 ligases (3). BAP1 binds BRCA1-associated RING domain 1 (BARD) and therefore inhibits BRCA1 autoubiquitination modulating E3 activity of BRCA1/BARD1 (4); and BAP1-deficient cells are sensitive to ionizing radiation and PARP inhibition (5, 6). In addition, we recently described that in the presence of wild-type (WT) BAP1, the expression of an alternative splice isoform of BAP1 (BAP1Δ) that lacks part of the catalytic domain, sensitizes cells to PARP inhibition, likely by competing with full-length BAP1 for complex formation (7).

BAP1 is found in multiprotein complexes and it takes part in several cellular processes including gene expression regulation (8). For example, BAP1 dimers are found to form two different complexes with the chromatin binders ASXL1 and ASXL2, human homologs of *Drosophila* additional sex combs (ASX), which both are able to deubiquitinate monoubiquitynated histone 2A (H2Aub1; ref. 9). BAP1 homolog in *Drosophila*, Calypso, in a complex with ASX is responsible for repression of HOX genes by maintaining H2A deubiquitinated in embryo while increasing HOX expression in particular tissues (10). The integrative molecular characterization of mesothelioma confirmed a significant change in transcriptional profile in samples with loss of function of *BAP1* (11) and a role for BAP1 in H2A ubiquitination-dependent transcription has been confirmed in mammalian cancer models (12). Therefore, although H2Aub1 is largely used to monitor

[1]Laboratory of Molecular Oncology, Lungen- und Thoraxonkologie Zentrum, University Hospital Zürich, Zürich, Switzerland. [2]Amsterdam UMC, Vrije Universiteit Amsterdam, Medical Oncology, Cancer Center Amsterdam, Amsterdam, the Netherlands. [3]Amsterdam UMC, Vrije Universiteit Amsterdam, Epidemiology and Biostatistics, Cancer Center Amsterdam, Amsterdam, the Netherlands. [4]Institute of Pathology and Molecular Pathology, University Hospital Zürich, Zürich, Switzerland. [5]Department of Thoracic Surgery, NKI, Amsterdam, the Netherlands. [6]Department of Thoracic Surgery, University Hospital Zürich, Zürich, Switzerland. [7]Lungen- und Thoraxonkologie Zentrum, University Hospital Zürich, 8091 Zürich, Switzerland. [8]Institute of Molecular Cancer Research, University of Zürich, Zürich, Switzerland.

BAP1 activity, it has an incompletely resolved and fine-tuning role in the control of gene expression.

In this study, using a genetically engineered MPM cell line pair expressing either functional or nonfunctional BAP1 in the same genetic background, we performed whole-genome siRNA screens assessing impaired survival. Silencing ribonucleotide reductase (RNR) subunits *RRM1* and *RRM2* conferred an increased lethality in *BAP1*-proficient cells. This observation was confirmed in a large panel of *BAP1*-proficient cells, including ($BAP1^{+/-}$) primary mesothelioma cells, which were more sensitive to RNR inhibition compared with *BAP1*-deficient. Our findings are consistent with a recent study investigating gemcitabine effects in two WT and two mutant BAP1 mesothelioma cell lines published while this manuscript was in preparation (13). In our study, we demonstrate that BAP1-dependent vulnerability of mesothelioma cells to RNR inhibition is linked to a repressor activity of BAP1 that is induced upon replicative stress.

Materials and Methods

Cell lines and primary culture

NCI-H226, NCI-H2452, and NCI-H2052 cell lines were obtained from the ATCC; ACC-Meso-1 and ACC-Meso-4 were from Riken BRC; Mero-82 were from European Collection of Cell Cultures; LP9/TERT-1 cell line was a kind gift of Dr. J. Rheinwald (Harvard Medical School, Boston, MA) Other cell lines and the primary culture SDM81 were established in our laboratory (7, 14). All cell lines were maintained in DMEM-F12 supplemented with 15% FCS and 1% penicillin/streptomycin solution. They were confirmed *Mycoplasma* free on a regular basis (PCR Mycoplasma Kit, MD Bioproducts). Cells were passaged for no longer than 2 months after thawing of early-passage stocks. NCI-H2452 and isogenic genetically recombined cell lines, LP9TERT-1, SPC111, NCI-H2052, MSTO-211H, SDM103T2, SPC111, ZL34, and NCI-H28, were authenticated by DNA fingerprinting of short tandem repeat loci (Microsynth). SDM81 cells were cultured and their genomic profile was assessed by copy number variation analysis and compared with the parental tumor as described previously (14). BAP1 sequence was confirmed to be WT in LP9/TERT-1 cells as described previously (7). Stably transfected cells were selected with puromycin. All cell lines were cultured at 37°C in a humidified 5% CO_2 incubator.

RNAi screen

High-throughput screening (HTS) was performed as described previously (15), using established automated liquid handling procedures. Three individual genome-wide screens were performed per cell line. Briefly, the siARRAY Human Genome library (Dharmacon, Thermo Fisher Scientific) comprising single-target pools of four distinct siRNAs was dispensed into 384-well plates (Greiner) at a concentration of 1.5 pmol in 10 μL 1× siRNA buffer (Dharmacon). siGENOME nontargeting control pool#1 and the siGENOME UBB SMARTpool siRNA (Dharmacon) were used as negative and positive control, respectively.

Plates were stored at −20°C until use. After thawing plates at room temperature, DharmaFECT 1 transfection reagent (Dharmacon) diluted in OptiMEM (GIBCO) was added to the wells using a Multidrop Combi (Thermo Fisher Scientific; final concentration 0.0125%). siRNA transfection complexes were allowed to form for 20 minutes to 2 hours. Then, 500 cells/well were plated in a volume of 55 μL of DMEM-F12 using a microFill cell dispenser (BioTek), resulting in a final siRNA concentration of 20 nmol/L and a final volume of 75 μL. After plating, cells were grown at normal cell culture conditions for

5 days, and then 6 μL CellTiter-Blue (Promega) was added into the wells. After 4-hour incubation, 15 μL of 6% SDS was added to stop the reaction and fluorescence (540Ex/590Em) was measured using a Tecan Infinite F200 microplate reader.

Selected hits were validated in deconvolution experiments in non-automated setup: four distinct siRNAs/gene were tested via viability assays and Western blotting using the same conditions and reagents as described above.

RNAi screen data analysis

Raw fluorescence data were processed in R (version 3.4.1 https://www.R-project.org/). Data were read into R using the cellHTS2 package. Subsequently, rscreenorm (16) was used to normalize the data, involving: log_2-transforming readouts for all the screens; calculating lethality scores relative to controls on plate according to the equation: lethality score = (median of $siRNA_x$ − median of siNon-Targeting)/(median siUBB − median siNonTargeting); and quantile normalizing lethality scores across screens. Identification of scores significantly different between cell lines was done by limma R package: siRNAs with FDR (Benjamini–Hochberg) corrected *P* values less than 0.05 were considered as displaying differential phenotype between the two cell lines.

RNA extraction, cDNA synthesis, and qPCR

RNA extraction, cDNA synthesis, and q-PCR were performed as described previously (17). Primers used for qPCR are listed in Supplementary Table S1.

Protein extraction and Western blotting

Total protein extracts were obtained by lysing the cells with hot Laemmli buffer (60 mmol/L Tris-HCl pH 6.8, 100 mmol/L DTT, 5% glycerol, 1.7% SDS) and passed through syringes (26G; ref. 18). Spheroids were collected 48 hours posttreatment. Protein concentration was determined using a Pierce 660nm Protein Assay (Thermo Fisher Scientific). Core histone extracts were prepared by acidic extraction as described previously (7), and their concentration was determined using Bradford protein assay. A total of 5 μg protein extract or 0.5 μg purified histones was separated on denaturing 10% or 15% SDS-PAGE gels and proteins were transferred onto PVDF membranes (0.45 μm, PerkinElmer). Membranes were probed with the following primary antibodies: mouse anti-BAP1 (C4, sc-28283), goat anti-RRM2 (E-16, sc-10846), mouse anti-p53 (DO-1, sc-126), and mouse anti-E2F-1 (KH95, sc-251) obtained from Santa Cruz Biotechnology; rabbit anti-histone H2A (ab18255), rabbit anti-RRM1 (EPR8483, ab137114), and rabbit anti-phospho-KAP1 (Ser824, ab70369) purchased from Abcam; rabbit anti-phospho-p53 (Ser15, no.9284) and anti-Ubiquitin (P4D1, no. 3936) obtained from Cell Signaling Technology; rabbit anti–phospho-BAP1 (Ser592, no. 93733) and mouse anti-γH2AX (Ser139, JBW30, no. 05-636) purchased from Millipore; rabbit anti-H3 (Poly6019) obtained from BioLegend; and mouse anti-β-actin (C4, MP691002) purchased from MP Biomedicals. Membranes were then incubated with one of the following secondary antibodies: rabbit anti-mouse IgG-HRP (no. A9004), goat anti-rabbit IgG-HRP (no. A0545), or rabbit anti-goat IgG-HRP (no. A5420), obtained from Sigma Aldrich. The signals were detected by enhanced chemiluminescence (Clarity TM ECL Substrate, Bio-Rad) and detected by Fusion Digital Imager (Vilber Lourmat).

BAP1 cloning, sequencing, and transfection

For isogenic BAP1 cell lines used in the screen, NCI-H2452 cells were transfected with pCI-puro_BAP1_WT (Addgene #68365) using

Lipofectamine 2000 reagent (Thermo Fisher Scientific) according to the manufacturer's instruction (7). For further experiments, NCI-H2452 cells or SDM81 primary cultures were stably transfected with either control empty vector, pCI-puro_BAP1_WT (Addgene #108439) or pCI-puro_BAP1_C91A (Addgene #108438). To obtain specific nonsynonymous mutations within the *BAP1* gene, the Quik-Change II Site-Directed Mutagenesis Kit (Stratagene) was used. All inserts were validated by sequencing and all primers are indicated in Supplementary Table S1.

RNA interference and drug treatment

To downregulate BAP1 expression, ON-TARGETplus SMARTpool or single siRNAs against *BAP1* or siGENOME nontargeting siRNA pool #1 and DharmaFECT 1 transfection reagent were obtained from Dharmacon. For RRM1 and RRM2 knockdown efficiency validation in MPM cell lines, pools of the two best distinct siRNAs against *RRM1* (siRRM1 #3 and #4) and *RRM2* (siRRM2 #1 and #3) were used at the same concentration as in the screen. Briefly, siRNA dissolved in 1× siRNA buffer (Dharmacon) was combined with transfection reagent dissolved in OptiMEM (final concentration 0.042%) and incubated for 20 minutes. Then, cells resuspended in normal growth medium were added to the siRNA/DharmaFECT 1 mixture and seeded onto plates, allowing for a final siRNA concentration of 20 nmol/L. A total of 0.5×10^5 cells (12-well plate) were plated for whole-cell protein lysates as wells as RNA extraction. Forty-eight hours later, cells were treated with either gemcitabine or hydroxyurea and after another 48 hours, protein lysates were prepared. Cell viability was assessed by MTT assay as described previously (14). Rescue of gemcitabine toxicity by deoxyribonucleoside monophosphates (dNMP) was assessed by treatment of the cells during 1 hour, followed by medium removal and addition of normal medium containing 100 μmol/L dNMP (Sigma Aldrich). Olaparib (AZD2281, Ku-0059436) was purchased from Selleckchem; gemcitabine was obtained from Lilly, and hydroxyurea from AppliChem.

Clonogenic and spheroid viability assays

Colony formation assays were performed as follows: NCI-H2452 clonal or SDM81 primary cells were plated at a density of 1,000/well in 6-well plates and subjected to treatment with different concentrations of a specific drug after 1 and 5 days. After another 5 days, cells were fixed and stained with Crystal violet.

Spheroids formation assays were performed as described previously (19). At day 4 after seeding, the spheroids were treated continuously with the drugs (0.01, 0.1, 1.0, 10.0, 100.0, and 500 μmol/L gemcitabine or 0.1, 0.5, 2.0 mmol/L hydroxyurea or remained untreated) for 6 days, and viability was analyzed using the CellTiter-Glo Luminescent Cell Viability Assay (Promega). For protein and RNA extraction, 10 to 20 spheroids/conditions were pooled.

Statistical analysis

Statistical analysis was performed using GraphPad Prism version 5.04 or SPSS V25. Differences with $P < 0.05$ were considered significant.

Results

Whole-genome RNAi screen reveals genetic vulnerabilities in BAP1-proficient cells

To identify genes whose inhibition induces synthetic lethality specifically in BAP1 loss-of-function MPM cells, we generated isogenic *BAP1*-proficient and *BAP1*-deficient cell lines by stably transfecting

the NCI-H2452 *BAP1*[A95D/−] (20, 21) cell line with either a *BAP1* WT expression vector or an empty vector (EV; Supplementary Fig. S1A). NCI-H2452 cells were selected on the basis of the fact that these cells express low levels of mutated BAP1 as compared with other mesothelioma cell lines (**Fig. 1A**). Multiple independent *BAP1*-proficient clones were generated and characterized by H2Aub1 levels, as well as by their response to olaparib in comparison to EV clonal cell lines. The selected BAP1-expressing clone was shown to exhibit similar growth characteristics as an EV clone (Supplementary Fig. S1B). In addition, BAP1 expression decreased H2Aub1 (**Fig. 1B**) as well as conferred resistance to olaparib (**Fig. 1C**), as we had previously observed using another cell line (7).

The final conditions (cell number per well, amount of DharmaFECT 1, concentration of siRNAs, incubation time for the screen as well as incubation time for the CellTiter-Blue readout) for the automated HTS setup were then optimized on the two clonal cell lines.

Three independent genome-wide screens per cell line were performed. After dispensing the siARRAY whole human genome library comprising single-target pools of four distinct siRNAs, as well as negative and positive control siRNAs into 384-well plates, the experiment began by adding transfection reagent and subsequently cells to the plates to allow reverse transfection (**Fig. 1D**). After 5 days, viability was measured by CTB assay and lethality score and significant hits were evaluated for *BAP1*-proficient versus deficient lines (**Fig. 1D**; Supplementary Fig. S1C). Differential lethality was then calculated between the two cell lines. Silencing 1,775 genes was found to significantly (based on $P < 0.05$ alone) differently affect viability of *BAP1*-proficient versus *BAP1*-deficient cells. Consistent with the clones' characterization, we observed a difference in lethality score of 0.12 and of 0.08 between the BAP1-proficient and deficient line for siPARP1 and for siPARP2, respectively. However, effects on viability were poor compared with effects of olaparib, likely because the drug inhibits both enzymes. From the list of 1,775 genes, we first considered the 191 genes where a differential lethality score ≥0.2 between the BAP1-proficient versus deficient line had been calculated. We searched for functional enrichment by gene ontology analysis using DAVID (22). Interestingly, using the Functional Annotation Clustering tool, the most enriched functional cluster was a group of terms associated with RNA splicing and processing (enrichment score, 4.23; Supplementary Table S2), which also had the highest score in a screen for genes involved in the so-called replicative stress (23), a term describing replication forks slowing or stalling by endogenously or exogenously derived impediments of DNA polymerases (24). We then took into account only genes with a differential lethality score ≤−0.3 or >0.3 and FDR < 0.05 between the BAP1-deficient versus proficient line (**Fig. 1E**). This revealed 11 significant differentially lethal genes (Supplementary Fig. S1D). Surprisingly, depletion of all the 11 hits was more cytotoxic to the *BAP1*-proficient cell line.

BAP1-proficient cells are more sensitive to RRM1 and RRM2 silencing

Two genes out of the 11 hits, namely *RRM1* and *RRM2*, encode the two subunits that together form a RNR protein heterotetramer (containing two copies of the catalytic subunit RRM1 and two copies of the regulatory subunit, RRM2), a key enzyme that converts ribonucleotide diphosphates (NDP) into deoxyribonucleotide diphosphates (dNDP), after which the NDP-kinase (NDPK) catalyzes the conversion of dNDPs to deoxyribonucleotide triphosphates (dNTP; ref. 25). Because RNR is of particular clinical relevance, as a drug targeting this enzyme is already used in second-line therapy in mesothelioma, we decided to focus on *RRM1* and *RRM2* for further
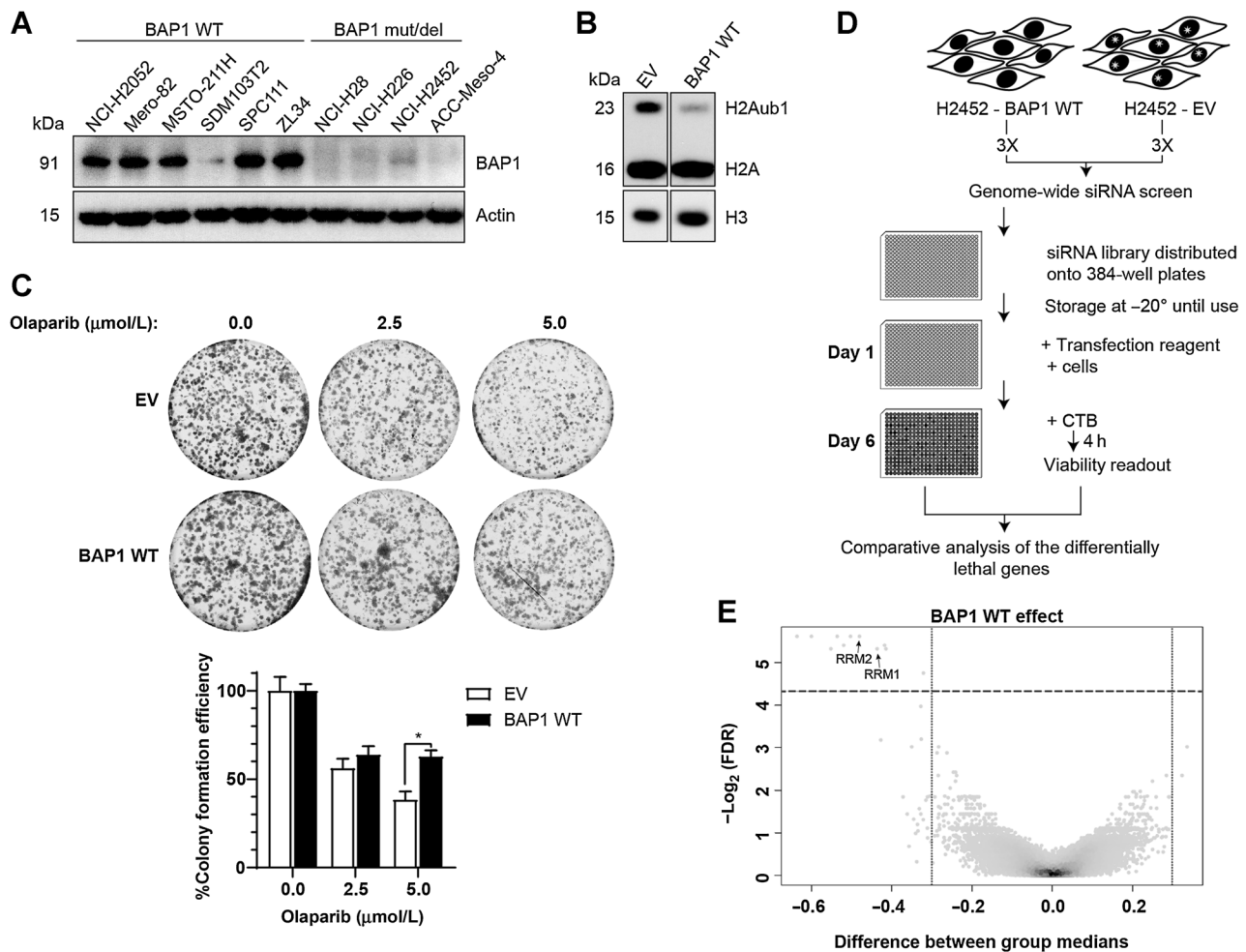
Figure 1.
Generation of isogenic BAP1-proficient and BAP1-deficient cell lines and genome-wide RNAi screen. **A,** Abundancy of BAP1 in a panel of MPM cell lines expressing either *BAP1* WT or *BAP1* mut/del. **B,** Anti-H2A and -H3 Western blot analysis performed on histone extracts obtained from clonal NCI-H2452 cell lines transfected with either empty vector (EV) or *BAP1* WT (BAP1) expression vector. **C,** Response to olaparib of clonal NCI-H2452 cell lines transfected with either empty vector (EV) or WT *BAP1* (BAP1) expression vector tested by clonogenic assay. **D,** Schematic representation of the RNAi screen setup. Three independent genome-wide screens per cell line were performed on isogenic BAP1-proficient and BAP1-deficient cell lines. Briefly, cells were reverse transfected with the siARRAY whole human genome library comprising single-target pools of four distinct siRNAs, as well as negative and positive control siRNAs, in 384-well plates. After 5 days, viability was measured by CTB incubation and reading fluorescence. Differential lethality scores were calculated between the two cell lines. **E,** Volcano plot of lethality scores in *BAP1*-proficient versus *BAP1*-deficient clonal cell lines. The *x*-axis specifies the difference in lethality scores between the two groups and the *y*-axis specifies the negative logarithm to the base 2 of the FDR. Hit selection criteria are highlighted by the lines (horizontal dashed line: FDR < 0.05; two vertical dotted lines: differential lethality score at ≤0.3 and >0.3). Besides the two genes (RRM1 and RRM2) that were further investigated in this study, the other 9 significant candidate genes are described in Supplementary Fig. S1D.

characterization. The genome-wide RNAi library comprises pools of four individual siRNAs per gene. Therefore, we deconvoluted each siRNA pool used in the screen for these 2 hits to exclude possible false-positive effects (26). We investigated the effect of individual siRNAs on overall lethality as well as BAP1-dependent lethality. Viability assays were performed with four individual siRNAs targeting either *RRM1* (siRRM1 #1, #2, #3, #4) or *RRM2* (siRRM2 #1, #2, #3, #4; **Fig. 2A**). The best *RRM1* and *RRM2* knockdown efficiency was obtained with siRRM1 #3 and #4 and siRRM2 #1 and #3 (Supplementary Fig. S2A and S2B). Moreover, as observed previously in the original screens, the *BAP1* WT expressing clonal cell line was significantly more sensitive to *RRM1* or *RRM2* depletion than the EV clonal cell line (**Fig. 2A**).

We then aimed at verifying the effect of *RRM1* or *RRM2* depletion in a broader panel of MPM cell lines. Four cell lines representing the *BAP1* WT group (SPC111, ACC-Meso-1, NCI-H2052, and Mero82; ref. 7) and three *BAP1* mutated or deleted (mut/del) cell lines [NCI-H226 (27), NCI-H2452, ACC-Meso-4 (21)] were transfected with a pool of the two siRNAs targeting *RRM1* or *RRM2* mentioned above, and the efficiency of the knockdown in all cell lines was assessed (Supplementary Fig. S2C and S2D). Interestingly, we noticed that silencing either *RRM1* or *RRM2* upregulates the expression of the other subunit in all cell lines, consistent with a reciprocal coregulation (28). We then assessed viability upon silencing. MPM cell lines expressing *BAP1* WT demonstrated decreased viability upon *RRM1* and *RRM2* knockdown compared with cells with *BAP1* mut/del status (**Fig. 2B**),
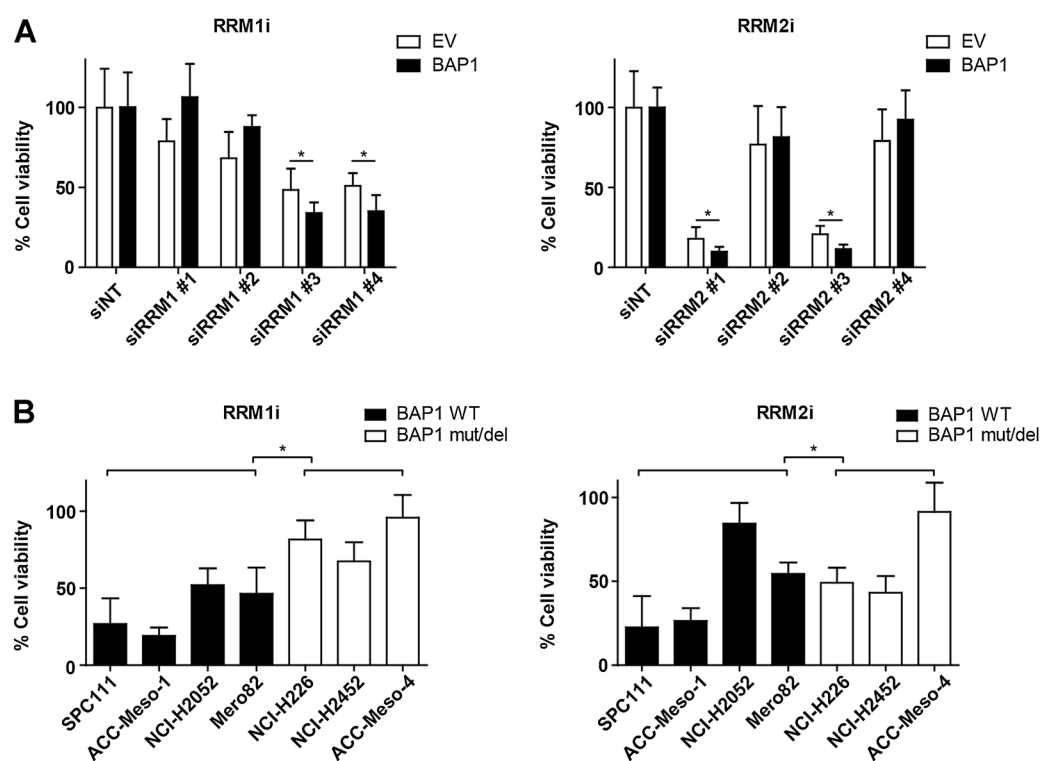
Figure 2.
RRM1 and RRM2 knockdown is more lethal in BAP1-proficient cell lines. **A,** Deconvolution of siRRM1 and siRRM2 pools used in the screen performed on the same isogenic cell lines as in original screens. Single siRNAs targeting *RRM1* or *RRM2* were tested via cell viability assay. **B,** Two best single siRNAs for *RRM1* and *RRM2* were pooled and tested on a panel of MPM cell lines via cell viability assay. *BAP1* WT cell lines (NCI-H2052, ACC-Meso-1, Mero82, and SPC111) are represented in black bars and *BAP1* mut/del cell lines (ACC-Meso-4, NCI-H226, NCI-H2452) in white bars. Data shown are relative to the siNon-Targeting control (siNT). Significance was determined by Mann–Whitney U test (*, $P < 0.05$).

suggesting higher sensitivity to siRNA-mediated depletion of RRM1 and RRM2. Noteworthy, expression of RRM1 as well as RRM2 was generally lower in *BAP1* WT positive MPM cell lines on both mRNA and protein level compared with the *BAP1* mut/del MPM cell lines (Supplementary Fig. S3A and S3B), although this was not particularly associated with different growth rates. Publicly available TCGA mRNA expression data of 87 MPM samples revealed that a similar inverse relationship between *BAP1* and *RRM1* or *RRM2* exists in clinical samples as well (Supplementary Fig. S3C). Overall, these data provide evidence that sensitivity of MPM cells to *RRM1* or *RRM2* depletion might depend on *BAP1* status, *BAP1* WT cell lines being more vulnerable.

BAP1-proficient cells are more sensitive to RRM1 and RRM2 inhibition in 2D and 3D

Because there are known selective inhibitors of RRM1 and RRM2, namely gemcitabine and hydroxyurea, respectively, which are already used in the clinic, we tested their effect on the growth of MPM cell lines.

First, we used isogenic SDM81 cells stably transfected with either EV, or *BAP1* WT or *BAP1* C91A a previously described catalytic dead mutant (Supplementary Fig. S4A; ref. 29). SDM81 primary culture is characterized by an almost haploid genome as parental tumor (**Fig. 3A**) and expresses WT BAP1 (Dr. Oehl, personal communication). Overexpression of *BAP1* C91A led to resistance to gemcitabine (**Fig. 3B**).

Silencing of *BAP1* in *BAP1* WT SPC111 and Mero-82 cells resulted in an increased expression of RNR on protein as well as on mRNA level

upon treatment of the cells with gemcitabine or hydroxyurea (**Fig. 3C**; Supplementary Fig. S4B). DNA damage upregulates RRM2 at least partially via upregulation of E2F transcription factor 1 (E2F-1; ref. 30). Therefore, we investigated expression of the latter and observed indeed increased levels of E2F-1 upon drug treatment in BAP1 knockdown cells (**Fig. 3D**).

Interestingly, drug treatment led to a decrease of BAP1 protein, but levels of mRNA were not significantly affected (**Fig. 3C**; Supplementary Fig. S4B).

Finally, to confirm that BAP1-dependent sensitization to cell death induced by gemcitabine involves *RRM2* expression, we silenced *BAP1* and/or *RRM2* in *BAP1* WT Mero-82 cells (**Fig. 3E**) and observed that BAP1 silencing reverted cell death induced by siRRM2 and gemcitabine (**Fig. 3F**).

Altogether, these results suggest that BAP1 DUB activity plays a crucial role in the mechanism of the observed sensitization and put forward the hypothesis of haploinsufficiency of BAP1 when the WT allele is expressed in the presence of a mutant allele.

To better mimic *in vivo* conditions, *BAP1* WT and *BAP1* mut/del cell lines were grown in spheroids (19) and subsequently treated with various concentrations of gemcitabine or hydroxyurea. Consistent with the effect of RRM1 silencing, gemcitabine was approximately 1000-fold more potent in decreasing cell viability in the *BAP1* WT group (**Fig. 4A** and **C**).

A similar effect was observed in spheroids treated with hydroxyurea, where the most evident separation in lethality between the two groups was detected at the concentration of 2 mmol/L (**Fig. 4B**

Figure 3.
RNR inhibition resistance and induction of RRM2 upregulation is higher in BAP1-deficient cells. **A,** Circos whole-genome copy number (CN) variations view of SDM81 tumor and primary cell culture. Light blue, CN gains; dark blue, high copy gains; red, CN losses. **B,** Response to gemcitabine of SDM81 primary mesothelioma cells expressing *BAP1* WT or *BAP1* C91A-mutant (C91A) or carrying an empty vector (EV) tested by clonogenic assay. **C,** SPC111 (*BAP1* WT) cell line was transfected with either siNT or siBAP1 and then treated with 0.1 μmol/L gemcitabine or 0.2 mmol/L hydroxyurea or remained untreated (Ctrl). Protein and RNA were extracted after 48 hours. Representative blot (left); and quantification of BAP1, RRM1, and RRM2 protein expression (right) and of *RRM1, RRM2,* and *BAP1* mRNA expression (bottom). Data are presented relative to the siNon-Targeting control-treated cells (siNT Ctrl) and are means ± SEM from 5 to 7 independent experiments. Significance was determined by Student *t* test or Wilcoxon paired tests (*, $P < 0.05$). **D,** E2F-1 protein expression. Data are normalized against actin and shown relative to siNT Ctrl. They are the means ± SD from 4 independent experiments. **E,** Western blot analysis of proteins extracted from Mero-82 cells upon silencing of *BAP1* and/or *RRM2*. **F,** Mero-82 cell viability assay upon silencing of *BAP1* and *RRM2* in the presence of two concentrations of gemcitabine.
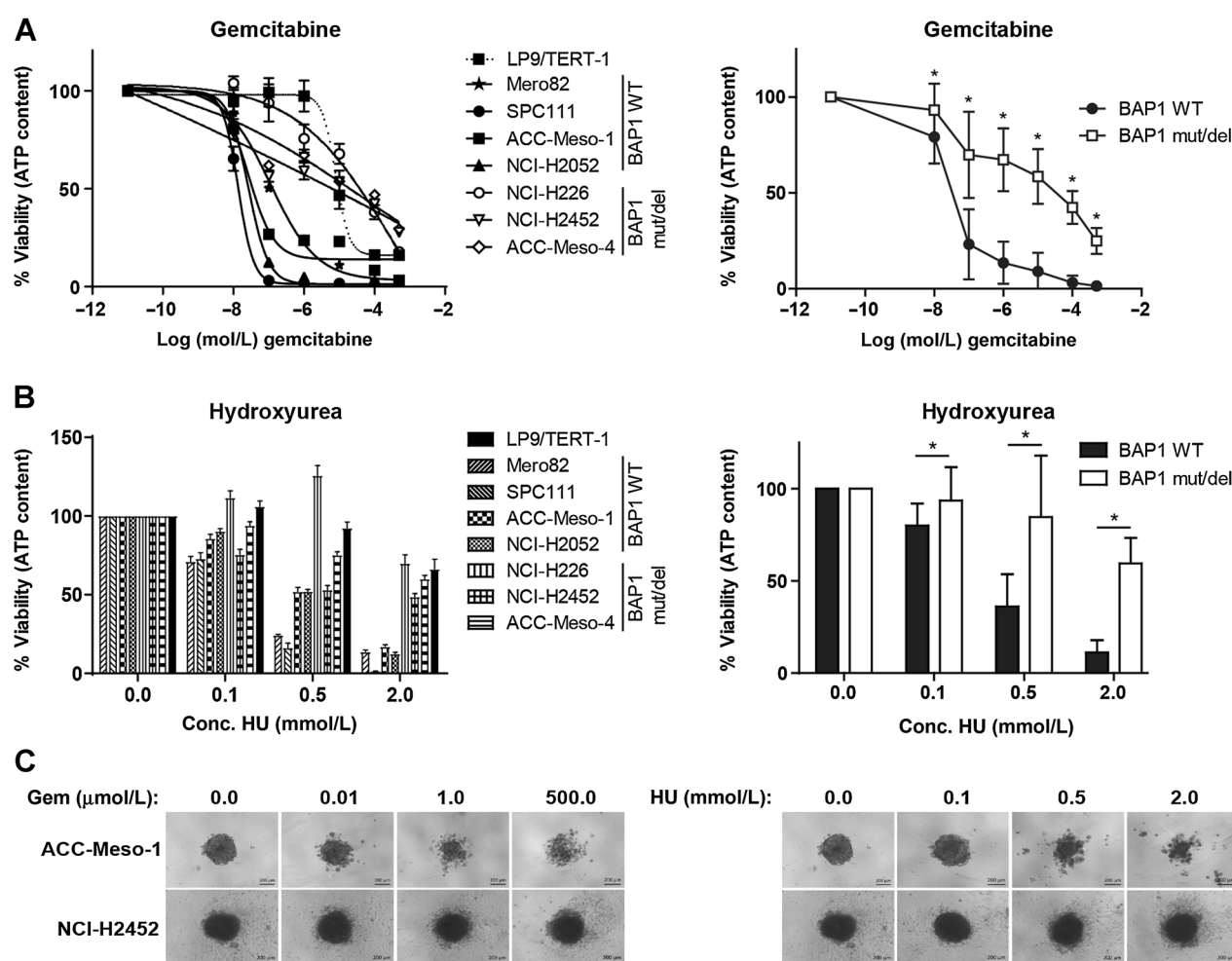
Figure 4.
BAP1-proficient MPM cell line sensitivity to RNR inhibition is maintained in 3D. Spheroids obtained from *BAP1* WT cell lines (NCI-H2052, ACC-Meso-1, Mero82, SPC111) and *BAP1* mut/del cell lines (ACC-Meso-4, NCI-H226, NCI-H2452) or normal mesothelial cells LP9/TERT-1 were treated with 0.01, 0.1, 1, 10, 100, or 500 μmol/L gemcitabine or 0.1, 0.5, or 2 mmol/L hydroxyurea or remained untreated. **A,** Quantification of ATP content after 6 days of gemcitabine treatment (left). Data are presented as mean ± SEM from ≥3 independent experiments. Pooled means from BAP1-proficient versus BAP1-deficient cell lines (right, mean ± SD). **B,** Quantification of ATP content after 6 days of hydroxyurea treatment (left). Data are presented as mean ± SEM from ≥3 independent experiments. Pooled means from *BAP1*-proficient versus *BAP1*-deficient cell lines (right, mean ± SD). Significance was determined by Mann–Whitney U test (*, $P < 0.05$). **C,** Representative spheroids treated with either gemcitabine or hydroxyurea.

and **C**). As expected, both gemcitabine and hydroxyurea had only minor effect on normal mesothelial LP9/TERT-1 cells, decreasing viability only at the highest concentrations (**Fig. 4A** and **B**).

Taken together, these data provide confirmation of the previous findings in 2D, that *BAP1* WT positive MPM cells are more sensitive to RRM1 and RRM2 inhibition.

To verify whether decreased expression of RRM1 and RRM2 observed in 2D conditions was maintained in 3D, thereby potentially underlying the differential sensitivity of MPM spheroids to RNR inhibition, we assessed RRM1 and RRM2 expression at baseline and upon drug treatment. Contrarily to the observation in 2D, in 3D, there was no obvious differential expression of RRM1 and RRM2 between BAP1 WT and BAP1 mut/del groups under basal conditions (**Fig. 5A**). In addition, we observed no clear differential pattern in RRM1 expression upon treatment, most likely due to the induction of ubiquitination and degradation of RRM1 upon gemcitabine treatment (31). However, expression of RRM2 was significantly more

upregulated upon gemcitabine and hydroxyurea treatment in *BAP1* mut/del compared with *BAP1* WT group. Although we did not measure cellular dNTP pools and previous studies showed no dNTP depletion upon hydroxyurea in mammalian cells (32), we assume that gemcitabine caused nucleotide depletion because supplementation of dNMP rescued its toxicity (Supplementary Fig. S4C). Decreasing the deoxynucleotide pool leads to slowing or stalling of the replication forks and loss of polymerase processivity leading to formation of a tract of single-stranded DNA causing genetic instability resulting in H2AX phosphorylation (referred as γH2AX; ref. 33). Therefore, we tested the level of γH2AX, as well as phospho KRAB associated protein-1 (pKAP1), two downstream targets of the kinase Ataxia telangiectasia mutated (ATM), and therefore being indicative of replicative stress. γH2AX levels were higher in the treated samples (**Fig. 5B**). Similarly, pKAP1 levels were upregulated upon both gemcitabine and hydroxyurea treatment. P53 was phosphorylated and stabilized upon gemcitabine and hydroxyurea treatment, indicating replicative stress in
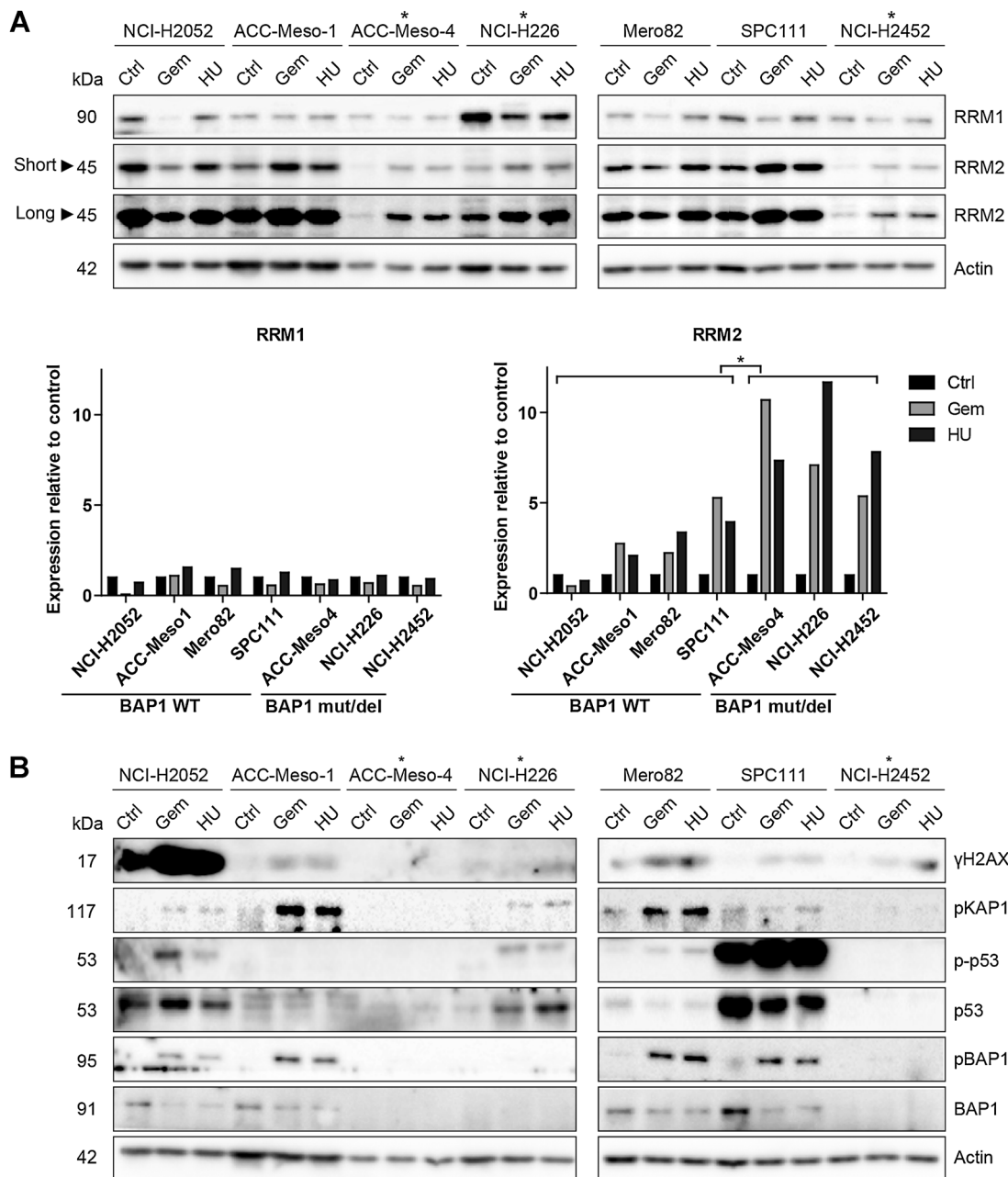
Figure 5.
RNR inhibition–induced RRM2 upregulation is higher in BAP1 mut/del cell lines and is accompanied by lower levels of residual DNA damage response. Spheroids obtained from *BAP1* WT cell lines (NCI-H2052, ACC-Meso-1, Mero82, SPC111) and *BAP1* mut/del cell lines (ACC-Meso-4, NCI-H226, NCI-H2452 marked with *) were treated with 10 µmol/L gemcitabine or 2 mmol/L hydroxyurea or remained untreated (Ctrl). Protein extracts were made after 48 hours and analyzed by Western blotting. **A,** Western blot analysis of RRM1 and RRM2 expression and quantification (average of two independent experiments) of RRM1 and RRM2 expression was normalized against actin and the data shown are relative to the controls (Ctrl). Blots shown are representative examples of two independent experiments. Significance was determined by Mann–Whitney *U* test (*, $P < 0.05$). **B,** Expression of DNA damage response markers: γH2AX, pKAP1 phospho-p53 (Ser15, p-p53), total p53, phospho-BAP1 (Ser592, pBAP1), and total BAP1.

concordance with γH2AX levels (**Fig. 5B**). We observed no p53 signal in the NCI-H2452 cell line, which has a mutation inducing a truncated p53 (34), and very low levels in ACC-Meso-1 and ACC-Meso-4, which have WT p53 (35).

Because BAP1 is phosphorylated in an ATM-dependent manner at S592 (36), we tested whether gemcitabine or hydroxyurea treatment had an impact on BAP1 S592 phosphorylation. As expected, pBAP1 was detectable in all *BAP1* WT cell lines upon treatment (**Fig. 5B**). Noteworthy, although the pBAP1 fraction was clearly elevated upon the treatment compared with the untreated cells, the total BAP1 level diminished in both gemcitabine and hydroxyurea treated *BAP1* WT spheroids.

Altogether, these data suggest that although DNA damage signaling was activated in both *BAP1*-proficient and deficient cells, *BAP1* mut/del cell lines are characterized by higher upregulation of RRM2 upon treatment as observed in 2D.

To exclude the possibility of the interplay of diverse genetic backgrounds in the tested cell lines, we used isogenic NCI-H2452 cell lines stably transfected with either EV, or *BAP1* WT or *BAP1* C91A expression vectors. We monitored BAP1 expression at protein level and observed that endogenous mutated BAP1 is phosphorylated under basal 2D conditions (Supplementary Fig. S4D), contrarily to what we had observed in basal conditions in 3D. BAP1 WT induced diminished levels of H2Aub1 (Supplementary Fig. S4E) and resistance to olaparib in colony formation assay (Supplementary Fig. S4F), in contrast to the C91A mutant, consistent with what has been previously reported (10, 29, 37). Subsequently, we tested the viability of the cells grown in spheroids upon gemcitabine or hydroxyurea treatment. As expected, cells expressing BAP1 WT, but not C91A mutant, are sensitized to gemcitabine compared with cells transfected with EV (**Fig. 6A**). The same observation was made for cells treated with hydroxyurea (**Fig. 6B**). Because the maximum sensitization effect of *BAP1* WT in these experiments was only 27%, we reasoned that this again might be due to competition between endogenous mutated BAP1 and exogenously expressed WT BAP1.

To further assess whether the same mechanisms was underlying BAP1 effects on sensitization to gemcitabine and hydroxyurea as we had observed in 2D, we tested whether *BAP1* WT reconstitution in NCI-H2452 cells would rescue these cells from high RRM2 upregulation. NCI-H2452 cells stably expressing either the *BAP1* WT or the C91A mutant or transfected with the EV control were grown in 3D and treated with gemcitabine or hydroxyurea for 48 hours. NCI-H2452 cells reconstituted with *BAP1* WT, but not the C91A mutant, showed a decreased induction of RRM2 expression compared with EV-transfected cells upon both treatments (**Fig. 6C**). This was accompanied by a significant decrease of basal expression of E2F-1 mRNA and protein in cells expressing *BAP1* WT (**Fig. 6D** and **E**).

Altogether, these data provide further evidence that *BAP1* mut/del cells react to replication stress-inducing agents with higher RNR upregulation compared with *BAP1* WT cells, suggesting an involvement of BAP1 in modulating E2F-1 and RNR increase under replicative stress conditions (Supplementary Fig. S5).

Discussion

In this study, we describe that *BAP1* loss induces chemoresistance to drugs inhibiting RNR activity in mesothelioma cells. This observation may have immediate clinical implications, as *BAP1* status could serve as a predictive biomarker for gemcitabine treatment in MPM.

Differential synthetic lethality between *BAP1*-proficient versus deficient cells included the RNR subunits RRM1 and RRM2 and we concentrated on understanding the underlying mechanisms because of the translational importance of this observation. RNR activity is necessary for DNA replication and repair. The activity of this enzyme is controlled at the transcriptional level during the cell cycle with maximal levels during S-phase. Although levels of RRM1 protein are almost constant in proliferating cells owing to a long half-life, the RRM2 protein is specifically degraded in late mitosis after polyubiquitination by the anaphase-promoting complex–Cdh1 ubiquitin ligase (reviewed in ref. 38).

It has been estimated that in 3D spheroids about one third of the cells are in quiescent state (39), corresponding better to the proliferation status of tumor cells (40) compared with 2D cell culture. Hence,

in this model, there are proliferating cells and nonproliferating cells, which could be less sensitive to the lack of deoxynucleotides. Nevertheless, using this system, we observed more than 3 log differences for the IC_{50} between BAP1-proficient and deficient cells. Quiescent cells still need deoxynucleotides for DNA repair and mitochondrial DNA synthesis, and a certain threshold concentration is necessary for some repair DNA polymerases (reviewed in ref. 38). Therefore, cells also express an alternative subunit having the same properties as RRM2, that is, RRM2B, which allows cells to produce enough deoxynucleotides in the absence of RRM2 (32). However, levels of RRM2B were very low even in the 3D model, and no significant changes were observed upon RRM1 and RRM2 inhibition.

Consistent with a previous study where silencing *RRM1* and *RRM2* caused genomic instability detectable through phosphorylation of histone variant H2AX (23), we observed activation of ATM in spheroids upon gemcitabine and hydroxyurea treatment. As expected, this led also to BAP1 phosphorylation because BAP1 is phosphorylated upon DNA damage on ATM and ATR consensus sites (36, 41). Ionizing radiation (IR) or hydroxyurea result in rapid phosphorylation of a small fraction of BAP1 at S592 in S-phase and dissociation from chromatin, to presumably regulate expression of DNA damage repair genes (42). In parallel to BAP1 phosphorylation, we observed a decrease of BAP1 protein levels, consistent with a previous study where BAP1 levels decreased after IR (43). Upon gemcitabine and hydroxyurea treatment, we could not detect any significant downregulation of BAP1 mRNA, while BAP1 protein levels were maintained in cells transfected with a WT *BAP1* expression plasmid. Therefore, we hypothesize that downregulation of BAP1 under conditions of genomic instability occurs at a post-transcriptional level, possibly by targeting the *BAP1* 3′UTR, which could be further investigated.

We observed a repressor role for BAP1 on *RRM2* expression in response to inhibition of RNR, when RRM1 and RRM2 are upregulated. This is in line with observations made on the NCI60 cell line panel (Supplementary Fig. S6A).

Upregulation of RRM1 and RRM2 is consistent with various studies showing that DNA-damaging agents increase the levels of RNR subunits (30, 44). In mammalian cells, upregulation of RRM2 after exposure of the cells to HU has been linked to decreased binding of Regulatory factor X (RFX) repressor to the RRM2 promoter (45). Therefore, a possible scenario is that RFX is more freely released in the absence of BAP1. Although RFX is not among previously reported BAP1 interactors (46), it might have been missed because this wide interactome study had been performed in the absence of replicative stress.

Another possibility is that BAP1 interacts with positive regulators of RRM2. RRM1 and RRM2 are part of the genes upregulated in retinoblastoma (Rb)-deficient mouse embryo fibroblasts (47). Rb negatively controls the activity of E2F transcription factors; hence, Rb could regulate RRM1 and RRM2 expression via E2F. Genotoxic stress upregulates RRM2 at least partially via upregulation of E2F-1 (30). The latter is stabilized downstream of ATM activity (48) and we also observed increased levels of E2F-1 upon silencing of BAP1 under replicative stress condition. E2F-1 is regulated by posttranslational modifications during cell-cycle progression and in response to DNA damage (reviewed in ref. 49) including by K63 ubiquitination; and UCH37, a member of the same DUB family as BAP1, has been shown to increase E2F-1 activity (50). In addition, BAP1 is known to bind Host Cell factor 1 (HCF-1) and the latter recruits activating methyltransferases to E2F-responsive promoters resulting in transcriptional activation of cell cycle–specific genes (51). However, although BAP1 deubiquitinates HCF-1 on K48-linked ubiquitin chains (52, 53),
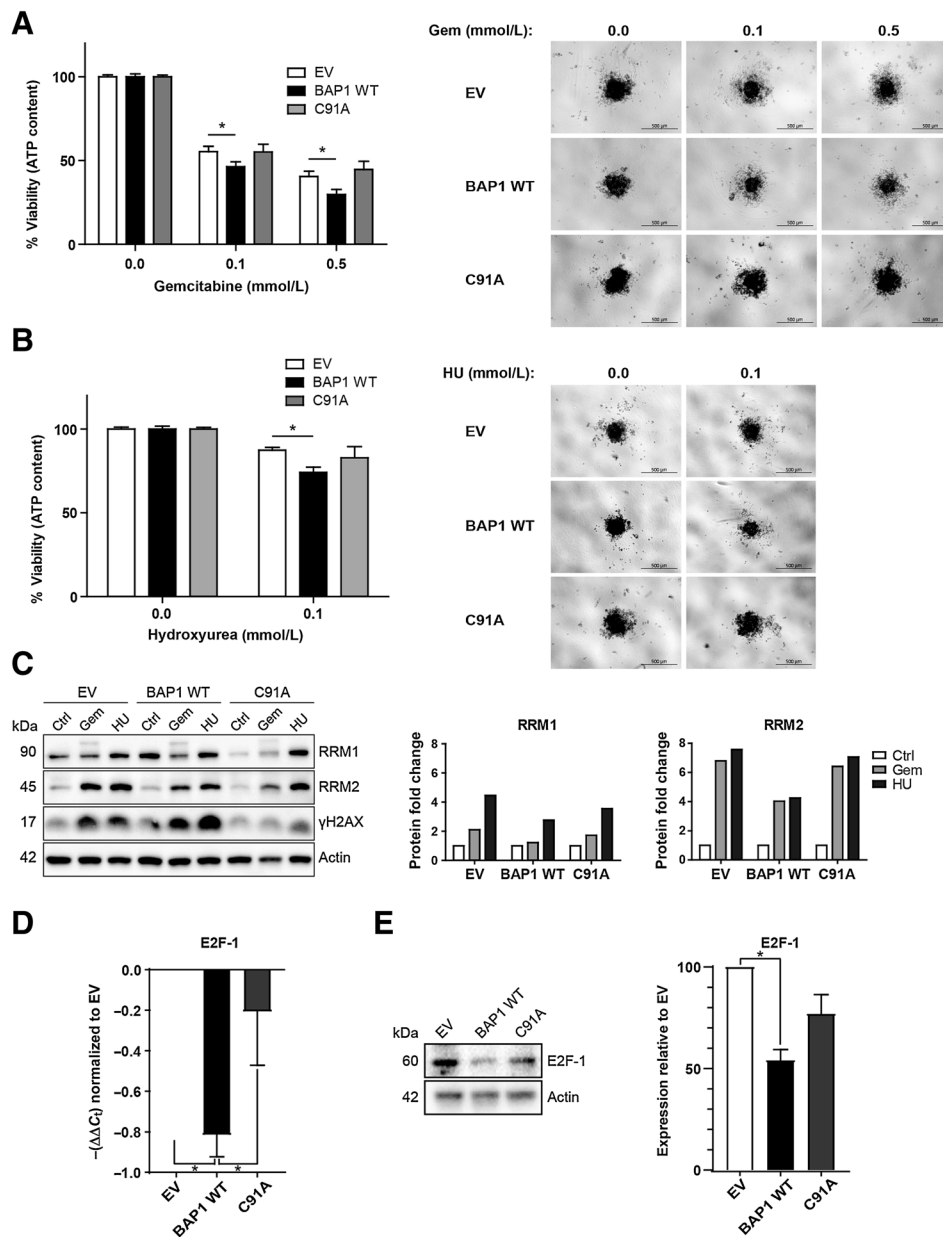
Figure 6.
Sensitivity of BAP1 WT MPM cells to RNR inhibition and RRM2 upregulation is dependent on its DUB activity. Spheroids obtained from NCI-H2452 stably expressing either *BAP1* WT or *BAP1* C91A mutant (C91A) or carrying an empty vector (EV) were treated with 0.1 or 0.5 mmol/L gemcitabine or 0.1 mmol/L hydroxyurea or remained untreated. **A,** Quantification of the ATP content after 6 days of treatment with gemcitabine relative to the control (left) and representative spheroids are presented (right). **B,** Quantification of the ATP content after 6 days of treatment with hydroxyurea relative to the control (left) and representative spheroids are shown (right). Data are presented as mean ± SEM from three independent experiments. Significance was determined by Mann–Whitney *U* test (*, $P < 0.05$). **C,** Spheroids obtained from NCI-H2452 stably expressing *BAP1* WT or *BAP1* C91A mutant (C91A) or carrying an empty vector (EV) were treated with 10 μmol/L gemcitabine or 2 mmol/L hydroxyurea or remained untreated (Ctrl) for 48 hours. Protein extracts were then analyzed by Western blotting and probed for RRM1, RRM2, and γH2AX. Western blot (left) and Western blot quantification of RRM1, RRM2 expression (right). Data are the mean from two independent experiments, normalized against actin and shown relative to the controls (Ctrl). **D,** Quantification of *E2F-1* mRNA expression from spheroids obtained from NCI-H2452 stably expressing *BAP1* WT or *BAP1* C91A mutant (C91A) or carrying an empty vector (EV). Data are the mean ± SD from three independent experiments, shown relative to the empty vector (EV). Significance was determined by Student *t* test (*, $P < 0.05$). **E,** E2F-1 protein expression and quantification in lysates from spheroids obtained from NCI-H2452 stably expressing *BAP1* WT or *BAP1* C91A mutant (C91A) or carrying an empty vector (EV). Data are the mean ± SD from three independent experiments, normalized against actin and shown relative to the empty vector (EV). Significance was determined by Student *t* test (*, $P < 0.05$).

differential gene expression revealed a significant BAP1-dependent effect on RRM1 but not RRM2 upregulation (54) in U2OS cells synchronized at G_1–S. This contrasts with the inverse relationship that we have observed. One possible reason for the difference is that the detection of an influence of BAP1 in that study concerned mostly gene with highest expression at G_1–S stage, which do not include the S-phase gene RRM2. Another possible explanation is that Daou and colleagues in a very elegant study (55) have shown that silencing BAP1 delays S-phase progression in U2OS cells; therefore, downregulation of RRM1 may represent a consequence of cell-cycle change and not a direct effect of BAP1 on RRM1 expression. In our model, we show that there is no effect of BAP1 expression on cell proliferation; therefore, changes cannot be justified by cell-cycle changes. It is likely that the identification of RRM1 and RRM2 as BAP1-dependent targets in the screen, which was performed in the absence of any exogenously induced replicative stress, was due to the serendipitous choice of the model, where we sought for differences between BAP1-proficient versus deficient cells using 2D cultures, in which cells undergo a mild replicative stress leading to BAP1 phosphorylation.

BAP1 is a complex protein acting as gene expression activator or repressor depending on the context. Even within the same cells, BAP1 leads to activation or repression of different Forkhead Box K2 (FOXK2) target genes after forming a complex with FOXK2 (56). The question whether BAP1 would have any effect on RRM1 and RRM2 via interaction with HCF-1 upon replicative stress conditions remains open.

Finally, BRCA1 acts as a transcriptional coactivator of RRM2 (57), so BAP1 effects could be mediated by its interaction with BRCA1. However, as this mechanism of RRM2 regulation was observed in glioblastoma cells but not in another cancer cell type, it is less likely.

BAP1 suppression of RRM2 expression upon replicative stress is consistent with tumor suppressor activity of BAP1 since overexpression of RRM2 is mutagenic in mouse cells and promotes lung carcinogenesis (58). Interestingly, high levels of RRM1 and RRM2 expression are associated with worse overall survival in patients with MPM (Supplementary Fig. S6B), and it would be of interest to investigate whether this is associated with BAP1 status. BAP1 could be part of the tightly regulated mechanisms to keep RRM2 expression under control because BAP1 is downregulated and phosphorylated upon replicative stress and phosphorylation has been linked to dissociation from chromatin (see above).

As mentioned, gemcitabine is already part of second-line treatment of patients with MPM. Investigation of response according to BAP1 status will be assessed in current clinical trials (NCT02991482, EORTC-NAVALT19) to verify whether BAP1 status is a predictor of response to this therapy and whether it can serve as a response or stratification biomarker.

Disclosure of Potential Conflicts of Interest

Authors' Contributions

Conception and design: A. Okonska, V.W. van Beusechem, E. Felley-Bosco
Development of methodology: A. Okonska, R.X. de Menezes, V.W. van Beusechem, E. Felley-Bosco
Acquisition of data (provided animals, acquired and managed patients, provided facilities, etc.): A. Okonska, S. Bühler, V. Rao, M. Ronner, M. Blijlevens, I.H. van der Meulen-Muileman, M. Wipplinger
Analysis and interpretation of data (e.g., statistical analysis, biostatistics, computational analysis): A. Okonska, S. Bühler, V. Rao, R.X. de Menezes, K. Oehl, W. Weder, E. Felley-Bosco
Writing, review, and/or revision of the manuscript: A. Okonska, R.X. de Menezes, E.F. Smit, W. Weder, R.A. Stahel, V.W. van Beusechem, E. Felley-Bosco
Administrative, technical, or material support (i.e., reporting or organizing data, constructing databases): S. Bühler, I.H. van der Meulen-Muileman, R.X. de Menezes
Study supervision: E.F. Smit, R.A. Stahel, L. Penengo, E. Felley-Bosco

Acknowledgments

References

1. Yap TA, Aerts JG, Popat S, Fennell DA. Novel insights into mesothelioma biology and implications for therapy. Nat Rev Cancer 2017;17:475–88.
2. Farzin M, Toon CW, Clarkson A, Sioson L, Watson N, Andrici J, et al. Loss of expression of BAP1 predicts longer survival in mesothelioma. Pathology 2015; 47:302–7.
3. Komander D, Clague MJ, Urbe S. Breaking the chains: structure and function of the deubiquitinases. Nat Rev Mol Cell Biol 2009;10:550–63.
4. Nishikawa H, Wu W, Koike A, Kojima R, Gomi H, Fukuda M, et al. BRCA1-associated protein 1 interferes with BRCA1/BARD1 RING heterodimer activity. Cancer Res 2009;69:111–9.
5. Pena-Llopis S, Vega-Rubin-de-Celis S, Liao A, Leng N, Pavia-Jimenez A, Wang S, et al. BAP1 loss defines a new class of renal cell carcinoma. Nat Genet 2012;44: 751–9.
6. Yu H, Pak H, Hammond-Martel I, Ghram M, Rodrigue A, Daou S, et al. Tumor suppressor and deubiquitinase BAP1 promotes DNA double-strand break repair. Proc Natl Acad Sci U S A 2014;111:285–90.
7. Parrotta R, Okonska A, Ronner M, Weder W, Stahel R, Penengo L, et al. A novel BRCA1-associated protein-1 isoform affects response of mesothelioma cells to drugs impairing BRCA1-mediated DNA repair. J Thorac Oncol 2017;12: 1309–19.
8. Carbone M, Yang H, Pass HI, Krausz T, Testa JR, Gaudino G. BAP1 and cancer. Nat Rev Cancer 2013;13:153–9.
9. Sahtoe DD, van Dijk WJ, Ekkebus R, Ovaa H, Sixma TK. BAP1/ASXL1 recruitment and activation for H2A deubiquitination. Nat Commun 2016;7: 10292.
10. Scheuermann JC, de Ayala Alonso AG, Oktaba K, Ly-Hartig N, McGinty RK, Fraterman S, et al. Histone H2A deubiquitinase activity of the Polycomb repressive complex PR-DUB. Nature 2010;465:243–7.
11. Hmeljak J, Sanchez-Vega F, Hoadley KA, Shih J, Stewart C, Heiman DI, et al. Integrative molecular characterization of malignant pleural mesothelioma. Cancer Discov 2018;8:1548–65.
12. Zhang Y, Shi J, Liu X, Feng L, Gong Z, Koppula P, et al. BAP1 links metabolic regulation of ferroptosis to tumour suppression. Nat Cell Biol 2018;20:1181–92.
13. Guazzelli A, Meysami P, Bakker E, Demonacos C, Giordano A, Krstic-Demonacos M, et al. BAP1 status determines the sensitivity of malignant mesothelioma cells to gemcitabine treatment. Int J Mol Sci 2019;20. doi: 10.3390/ijms20020429.
14. Oehl K, Kresoja-Rakic J, Opitz I, Vrugt B, Weder W, Stahel R, et al. Live-cell mesothelioma biobank to explore mechanisms of tumor progression. Front Oncol 2018;8:40.

15. de Lange J, Faramarz A, Oostra AB, de Menezes RX, van der Meulen IH, Rooimans MA, et al. Defective sister chromatid cohesion is synthetically lethal with impaired APC/C function. Nat Commun 2015;6:8399.

16. Bachas C, Hodzic J, van der Mijn J, Stoepker C, Verheul H, Wolthuis R, et al. Rscreenorm: normalization of CRISPR and siRNA screen data for more reproducible hit selection. BMC Bioinformatics 2018;19:301.

17. Thurneysen C, Opitz I, Kurtz S, Weder W, Stahel RA, Felley-Bosco E. Functional inactivation of NF2/merlin in human mesothelioma. Lung Cancer 2009;64:140–7.

18. Kresoja-Rakic J, Kapaklikaya E, Ziltener G, Dalcher D, Santoro R, Christensen BC, et al. Identification of cis- and trans-acting elements regulating calretinin expression in mesothelioma cells. Oncotarget 2016;7:21272–86.

19. Echeverry N, Ziltener G, Barbone D, Weder W, Stahel RA, Broaddus VC, et al. Inhibition of autophagy sensitizes malignant pleural mesothelioma cells to dual PI3K/mTOR inhibitors. Cell Death Dis 2015;6:e1757.

20. Bott M, Brevet M, Taylor BS, Shimizu S, Ito T, Wang L, et al. The nuclear deubiquitinase BAP1 is commonly inactivated by somatic mutations and 3p21.1 losses in malignant pleural mesothelioma. Nat Genet 2011;43:668–72.

21. Hakiri S, Osada H, Ishiguro F, Murakami H, Murakami-Tonami Y, Yokoi K, et al. Functional differences between wild-type and mutant-type BAP1 tumor suppressor against malignant mesothelioma cells. Cancer Sci 2015; 106:990–9.

22. Huang da W, Sherman BT, Lempicki RA. Systematic and integrative analysis of large gene lists using DAVID bioinformatics resources. Nat Protoc 2009;4: 44–57.

23. Paulsen RD, Soni DV, Wollman R, Hahn AT, Yee MC, Guan A, et al. A genome-wide siRNA screen reveals diverse cellular processes and pathways that mediate genome stability. Mol Cell 2009;35:228–39.

24. Zeman MK, Cimprich KA. Causes and consequences of replication stress. Nat Cell Biol 2014;16:2–9.

25. Aye Y, Li M, Long MJ, Weiss RS. Ribonucleotide reductase and cancer: biological mechanisms and targeted therapies. Oncogene 2015;34:2011–21.

26. Echeverri CJ, Beachy PA, Baum B, Boutros M, Buchholz F, Chanda SK, et al. Minimizing the risk of reporting false positives in large-scale RNAi screens. Nat Methods 2006;3:777–9.

27. Jensen DE, Proctor M, Marquis ST, Gardner HP, Ha SI, Chodosh LA, et al. BAP1: a novel ubiquitin hydrolase which binds to the BRCA1 RING finger and enhances BRCA1-mediated cell growth suppression. Oncogene 1998;16: 1097–112.

28. Sagawa M, Ohguchi H, Harada T, Samur MK, Tai YT, Munshi NC, et al. Ribonucleotide reductase catalytic subunit M1 (RRM1) as a novel therapeutic target in multiple myeloma. Clin Cancer Res 2017;23:5225–37.

29. Ventii KH, Devi NS, Friedrich KL, Chernova TA, Tighiouart M, Van Meir EG, et al. BRCA1-associated protein-1 is a tumor suppressor that requires deubiquitinating activity and nuclear localization. Cancer Res 2008;68:6953–62.

30. Zhang YW, Jones TL, Martin SE, Caplen NJ, Pommier Y. Implication of checkpoint kinase-dependent up-regulation of ribonucleotide reductase R2 in DNA damage response. J Biol Chem 2009;284:18085–95.

31. Zhang Y, Li X, Chen Z, Bepler G. Ubiquitination and degradation of ribonucleotide reductase M1 by the polycomb group proteins RNF2 and Bmi1 and cellular response to gemcitabine. PLoS One 2014;9:e91186.

32. Hakansson P, Hofer A, Thelander L. Regulation of mammalian ribonucleotide reduction and dNTP pools after DNA damage and in resting cells. J Biol Chem 2006;281:7834–41.

33. Ewald B, Sampath D, Plunkett W. H2AX phosphorylation marks gemcitabine-induced stalled replication forks and their collapse upon S-phase checkpoint abrogation. Mol Cancer Ther 2007;6:1239–48.

34. Manfredi JJ, Dong J, Liu WJ, Resnick-Silverman L, Qiao R, Chahinian P, et al. Evidence against a role for SV40 in human mesothelioma. Cancer Res 2005;65: 2602–9.

35. Usami N, Fukui T, Kondo M, Taniguchi T, Yokoyama T, Mori S, et al. Establishment and characterization of four malignant pleural mesothelioma cell lines from Japanese patients. Cancer Sci 2006;97:387–94.

36. Stokes MP, Rush J, Macneill J, Ren JM, Sprott K, Nardone J, et al. Profiling of UV-induced ATM/ATR signaling pathways. Proc Natl Acad Sci U S A 2007;104: 19855–60.

37. Ismail IH, Davidson R, Gagne JP, Xu ZZ, Poirier GG, Hendzel MJ. Germline mutations in BAP1 impair its function in DNA double-strand break repair. Cancer Res 2014;74:4282–94.

38. Thelander L. Ribonucleotide reductase and mitochondrial DNA synthesis. Nat Genet 2007;39:703–4.

39. Daubriac J, Fleury-Feith J, Kheuang L, Galipon J, Saint-Albin A, Renier A, et al. Malignant pleural mesothelioma cells resist anoikis as quiescent pluricellular aggregates. Cell Death Differ 2009;16:1146–55.

40. Kadota K, Suzuki K, Colovos C, Sima CS, Rusch VW, Travis WD, et al. A nuclear grading system is a strong predictor of survival in epithelioid diffuse malignant pleural mesothelioma. Mod Pathol 2012;25:260–71.

41. Matsuoka S, Ballif BA, Smogorzewska A, McDonald ER III, Hurov KE, Luo J, et al. ATM and ATR substrate analysis reveals extensive protein networks responsive to DNA damage. Science 2007;316:1160–6.

42. Eletr ZM, Yin L, Wilkinson KD. BAP1 is phosphorylated at serine 592 in S-phase following DNA damage. FEBS Lett 2013;587:3906–11.

43. Ofir R, Zhang LC, Kyne AP, Houtzager V, O'Connor L, Adams JM. Gamma-radiation-induced growth arrest and apoptosis in p53-null lymphoma cells is accompanied by modest transcriptional changes in many genes. DNA Cell Biol 2000;19:29–37.

44. Lin ZP, Belcourt MF, Cory JG, Sartorelli AC. Stable suppression of the R2 subunit of ribonucleotide reductase by R2-targeted short interference RNA sensitizes p53 (-/-) HCT-116 colon cancer cells to DNA-damaging agents and ribonucleotide reductase inhibitors. J Biol Chem 2004;279:27030–8.

45. Lubelsky Y, Reuven N, Shaul Y. Autorepression of rfx1 gene expression: functional conservation from yeast to humans in response to DNA replication arrest. Mol Cell Biol 2005;25:10665–73.

46. Sowa ME, Bennett EJ, Gygi SP, Harper JW. Defining the human deubiquitinating enzyme interaction landscape. Cell 2009;138:389–403.

47. Markey MP, Bergseid J, Bosco EE, Stengel K, Xu H, Mayhew CN, et al. Loss of the retinoblastoma tumor suppressor: differential action on transcriptional programs related to cell cycle control and immune function. Oncogene 2007;26: 6307–18.

48. Lin WC, Lin FT, Nevins JR. Selective induction of E2F1 in response to DNA damage, mediated by ATM-dependent phosphorylation. Genes Dev 2001;15: 1833–44.

49. Biswas AK, Johnson DG. Transcriptional and nontranscriptional functions of E2F1 in response to DNA damage. Cancer Res 2012;72:13–7.

50. Mahanic CS, Budhavarapu V, Graves JD, Li G, Lin WC. Regulation of E2 promoter binding factor 1 (E2F1) transcriptional activity through a deubiquitinating enzyme, UCH37. J Biol Chem 2015;290:26508–22.

51. Tyagi S, Chabes AL, Wysocka J, Herr W. E2F activation of S phase promoters via association with HCF-1 and the MLL family of histone H3K4 methyltransferases. Mol Cell 2007;27:107–19.

52. Machida YJ, Machida Y, Vashisht AA, Wohlschlegel JA, Dutta A. The deubiquitinating enzyme BAP1 regulates cell growth via interaction with HCF-1. J Biol Chem 2009;284:34179–88.

53. Misaghi S, Ottosen S, Izrael-Tomasevic A, Arnott D, Lamkanfi M, Lee J, et al. Association of C-terminal ubiquitin hydrolase BRCA1-associated protein 1 with cell cycle regulator host cell factor 1. Mol Cell Biol 2009;29:2181–92.

54. Yu H, Mashtalir N, Daou S, Hammond-Martel I, Ross J, Sui G, et al. The ubiquitin carboxyl hydrolase BAP1 forms a ternary complex with YY1 and HCF-1 and is a critical regulator of gene expression. Mol Cell Biol 2010;30:5071–85.

55. Daou S, Hammond-Martel I, Mashtalir N, Barbour H, Gagnon J, Iannantuono NV, et al. The BAP1/ASXL2 histone H2A deubiquitinase complex regulates cell proliferation and is disrupted in cancer. J Biol Chem 2015;290:28643–63.

56. Okino Y, Machida Y, Frankland-Searby S, Machida YJ. BRCA1-associated protein 1 (BAP1) deubiquitinase antagonizes the ubiquitin-mediated activation of FoxK2 target genes. J Biol Chem 2015;290:1580–91.

57. Rasmussen RD, Gajjar MK, Tuckova L, Jensen KE, Maya-Mendoza A, Holst CB, et al. BRCA1-regulated RRM2 expression protects glioblastoma cells from endogenous replication stress and promotes tumorigenicity. Nat Commun 2016;7:13398.

58. Xu X, Page JL, Surtees JA, Liu H, Lagedrost S, Lu Y, et al. Broad overexpression of ribonucleotide reductase genes in mice specifically induces lung neoplasms. Cancer Res 2008;68:2652–60.